Applied Physics Express

LETTER

Fast and high light yield scintillation in the Ga_2O_3 semiconductor material

To cite this article: Takayuki Yanagida *et al* 2016 *Appl. Phys. Express* **9** 042601

Applied Physics Express **9**, 042601 (2016)
http://doi.org/**10.7567/APEX.9.042601**

Fast and high light yield scintillation in the Ga_2O_3 semiconductor material

Takayuki Yanagida*, Go Okada, Takumi Kato, Daisuke Nakauchi, and Satoko Yanagida

Graduate School of Materials Science, Nara Institute of Science and Technology, Ikoma, Nara 630-0192, Japan

*E-mail: t-yanagida@ms.naist.jp

Received February 13, 2016; accepted February 19, 2016; published online March 4, 2016

We report the distinct scintillation properties of the well-known Ga_2O_3 semiconductor material. Under UV excitation, the photoluminescence (PL) emission peak appeared near a wavelength of 380 nm with a quantum yield of 6%, and fast decays of 8 and 793 ns were observed. In contrast, the X-ray-induced scintillation spectrum showed an intense emission band near a wavelength of 380 nm, whose decay curve was reproduced using two exponential decay components with time constants of 8 and 977 ns. The pulse height spectrum of ^{137}Cs γ-rays measured using Ga_2O_3 showed a clear photoabsorption peak with a light yield of 15000 ± 1500 photons/MeV.

Radiation detectors have been utilized in many kinds of nondestructive investigations. In many such applications, a scintillation detector, which consists of a scintillator and a photodetector, is used. A scintillator is a type of a luminescent material that converts a high-energy ionizing radiation (photon or particle) to hundreds of visible photons via energy migration from the host matrix to the emission centers.[1)] Scintillators play an important role in many scientific and industrial fields, including astrophysics,[2)] particle physics,[3)] medical imaging,[4)] security,[5)] nuclear plants,[6)] and well-logging.[7)] In general, scintillation detectors can be classified into two types. The first type is based on the photon counting technique, which allows highly sensitive detection and the capability to resolve the radiation energy spectra using pulse height spectroscopy (PHS). The photon counting technique is generally used in high-energy physics industries. The second type is based on signal integration, which has the advantage of fast and high signal-to-nose measurements as long as the incident radiation is intense enough. This technique is mainly used in radiation imaging applications such as applications for airport security and medical imaging.

The scintillation process mainly involves two separate effects. The first effect is absorption of incident ionizing radiation, and another effect is emission of light. Therefore, typical scintillator materials are composed as a host matrix to absorb the radiation energy effectively and emission centers to emit light as scintillation. Nowadays, insulator materials doped using rare earth or transition metal ions are commonly used in practical applications.[8–12)] On the other hand, semiconductor crystals have also attracted attention due to their intrinsically high light yield and fast decay time without doping any emission centers.[13)] As *semiconductor scintillators*, several materials have been introduced such as Ga-doped ZnO, In-doped CdS, CuI, PbI_2, and HgI_2.[13,14)] Among these materials, CuI, PbI_2, and HgI_2 are not used in practical applications since they can only be operated at low temperatures. So far, in terms of practical applications, we have investigated GaN,[15)] ZnO,[16)] and CdS,[17)] and they are found to exhibit fast scintillation due to exciton emission. Particularly, ZnO has a great potential for practical use, and we have developed a photon counting-based two-dimensional imager using ZnO for monitoring charged particles.[18)] Furthermore, throughout the course of research, we noticed that In- and Ga-doped ZnO show an efficient scintillation response characterized by a high light yield and a fast decay time.[19)] Despite these advantages of ZnO, one of the drawbacks is that the fabrication of a bulk form with high density and homogeneity is challenging. Since most radiation types, such as X-rays and γ-rays, have a high penetrating power, these properties are essential for an efficient scintillator material to absorb the radiation energy effectively.

β-Ga_2O_3 semiconductor crystals are of our great interest to extend our knowledge and to discover new options of semiconductor scintillators. β-Ga_2O_3 is a recently developed and well-known semiconductor material.[20–26)] It has a relatively wide bandgap of 4.9 eV and a monoclinic structure with $C2/m$ space group containing both octahedral and tetrahedral cation sites in equal quantities.[20)] A β-Ga_2O_3 crystal can be fabricated with a large size and a single crystalline form using a melt-growth method. Typical applications of Ga_2O_3 are semiconductor photodetectors,[21)] field-effect transistors (FETs),[22)] and transparent electrodes.[23)] In this study, we investigated the scintillation properties of a β-Ga_2O_3 crystal since no reports were found on the scintillation responses of this material.

The Ga_2O_3 sample used in this study is a product of TAMURA, with a size of $10 \times 15 \times 0.65\,mm^3$. Throughout the course of research, the photoluminescence (PL), scintillation, and thermally stimulated luminescence (TSL) properties were comprehensively studied. The PL excitation-emission contour plot was measured using Hamamatsu Quantaurus-QY over the excitation wavelength range of 250–400 nm with an interval of 10 nm. The PL quantum efficiency was also measured using the same instrument. The PL decay time profile was measured using Hamamatsu Quantaurus-τ. The emission at a wavelength of 380 nm was measured under an excitation wavelength of 280 nm. The X-ray-induced scintillation spectrum was observed using our original setup. The excitation source was an X-ray generator supplied with a voltage of 80 kV and a tube current of 2.5 mA. Detailed information about the setup can be found elsewhere.[27)] The scintillation decay time profile was measured using an afterglow characterization system,[28)] which was equipped with a pulsed X-ray tube. The system integrates the emission signal over the wavelength range of approximately 160–650 nm. The obtained decay profile was approximated using a second-order exponential decay function, from which the two decay time constants were derived. PHS was implemented using a ^{137}Cs source and a photomultiplier tube (PMT; Hamamatsu R7600U-200). The detailed setup is explained elsewhere.[29)] Here, the absolute light yield was calibrated using Pr-doped LuAG as a standard sample since it showed a scintillation wavelength range of 310–400 nm, which is similar to that of Ga_2O_3.[30)] The absolute light yield of the

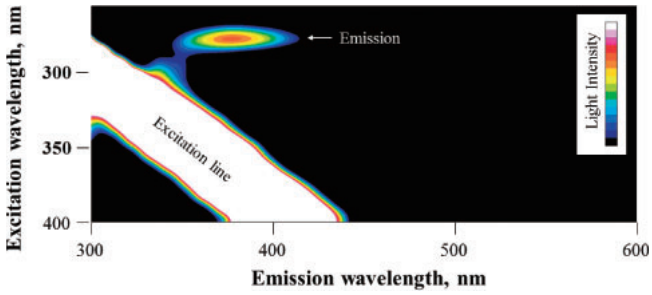

Fig. 1. Excitation (vertical axis) and emission (horizontal axis) map of Ga_2O_3.

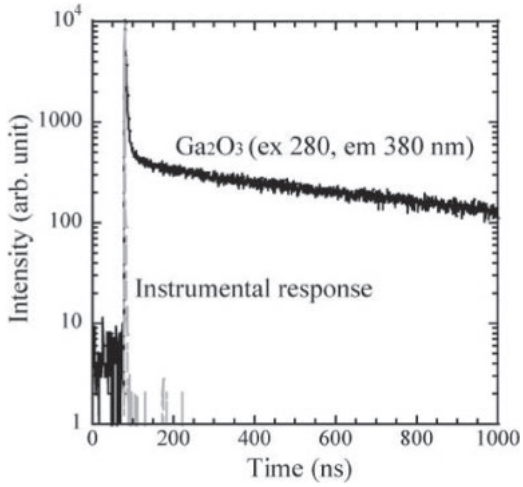

Fig. 2. PL decay time profile of Ga_2O_3 monitoring at a wavelength of 380 nm under an excitation wavelength of 280 nm.

latter material was previously accurately measured using an avalanche photodiode and a ^{55}Fe source.[30] The TSL glow curve was measured using Nanogray TL2000 with a heating rate of 1 °C/s.[31]

The PL excitation-emission contour plot is shown in Fig. 1. The PL emission was observed near a wavelength of 380 nm under the excitation wavelength range of 260–280 nm. The PL quantum yield was approximately 6%. In pioneering studies, the emission origin has already been well discussed. The emission band is mainly composed of two peaks in the UV and blue ranges. The origin of the UV emission was considered to be the recombination of free electrons and self-trapped holes.[32] On the other hand, the donor–acceptor recombination involving an oxygen vacancy, interstitial Ga, and Ga vacancies is considered to be the origin of the blue emission.[33,34] In our sample, the dominant emission was in the near UV region, and the blue emission was not clearly observed. Possibly, the blue emission was still present, but it overlapped with the tail of the UV emission band. Figure 2 shows the PL decay time profile of Ga_2O_3. The deduced decay times were 8 and 793 ns. This result is roughly consistent with the previously reported values, which are less than 30 ns with an afterglow on the order of hundreds of nanoseconds for the UV emission[35] and on the order of microseconds to milliseconds for the blue emission.[20,33] In our experiment, the latter slow emission component was not observed.

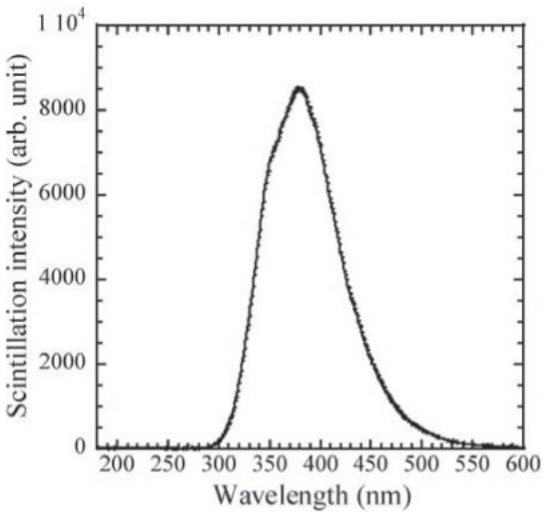

Fig. 3. X-ray-induced scintillation spectrum of Ga_2O_3.

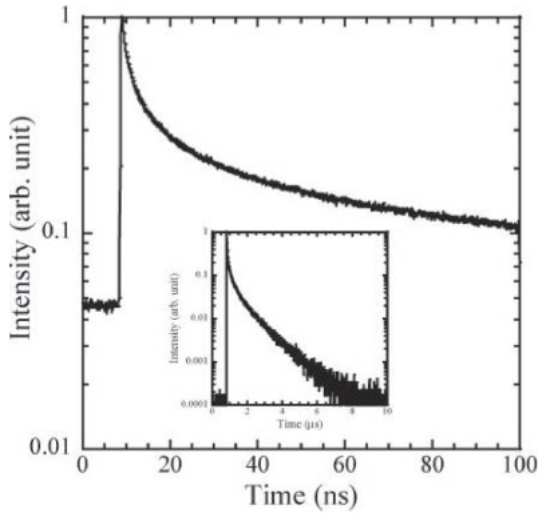

Fig. 4. X-ray-induced scintillation decay time profile of Ga_2O_3. The inset expands the time range to 10 μs to show the slower component.

Figure 3 represents the X-ray induced scintillation spectrum. The peak emission wavelength is approximately the same as that in PL, ~380 nm. The spectral range of this emission is consistent with most conventional PMTs. This is an advantage for practical applications. As far as we are aware, this is one of few scintillation semiconductor materials showing emission in this range besides GaN and ZnO. Figure 4 demonstrates the scintillation decay time profile of Ga_2O_3. The decay curve consists of two exponential components with time constants of 8 and 977 ns. The decay time of the faster component is the same as that in PL. Although some semiconductor scintillators show faster scintillation due to free exciton luminescence,[15,16] it is faster than that of common rare earth doped scintillators such as Ce-doped Lu_2SiO_5[37] and $Gd_3(Al,Ga)_5O_{12}$.[27] In contrast, the slower component is longer than that in PL. This is because PL indicates only the direct excitation and relaxation processes of the emission centers while the scintillation processes include some additional processes since the excitation energy is much larger than PL, and the number of generated charges is much greater.

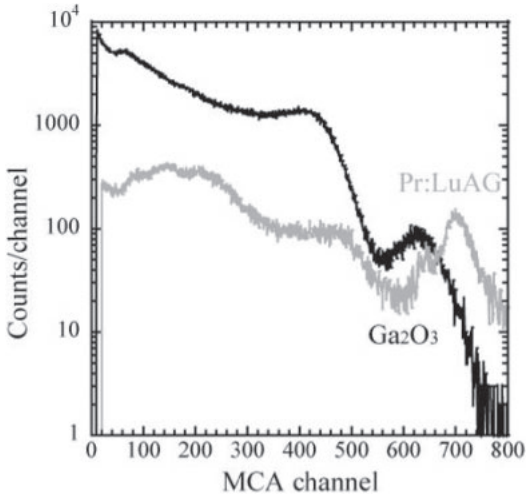

Fig. 5. ^{137}Cs γ-ray-irradiated pulse height spectrum of Ga_2O_3 and Pr-doped LuAG.

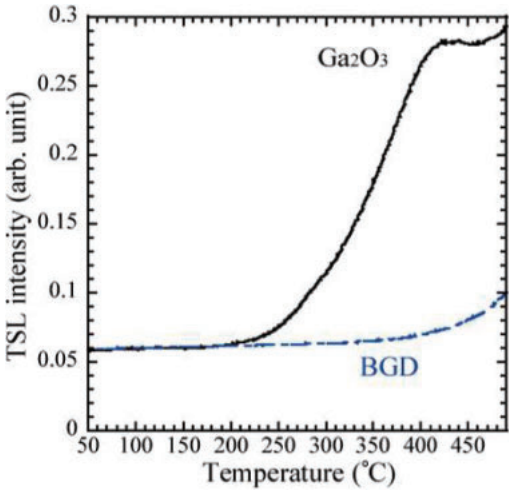

Fig. 6. TSL glow curve of Ga_2O_3 after irradiation with X-rays with a dose of 1 Gy. The background (BGD) signal measured without the sample is superposed.

The ^{137}Cs 662 keV γ-ray irradiated pulse height spectrum is presented in Fig. 5. Since the spectrum clearly illustrates the photoabsorption peak [~640 channel (ch)] and the Compton edge (~440 ch), the Ga_2O_3 semiconductor material can be used for γ-ray measurements based on PHS. Considering the quantum yield of the PMT and the peak channel of Pr-doped LuAG as a standard reference, the scintillation light yield of Ga_2O_3 was deduced to be 15000 ± 1500 photons/MeV. To the best of our knowledge, the clear detection of the photoabsorption peak using semiconductor scintillators is only possible in Te-doped CdS and ZnSe.[36] Compared to these materials, the light yield of Ga_2O_3 is superior to that of Te-doped ZnSe and comparable to that of Te-doped CdS. These Te-doped semiconductors are well compatible with photodiodes as their emission wavelengths are in the range of 600–800 nm.[36] Our Ga_2O_3 semiconductor scintillator is the best to be used with a PMT and is the only option among the semiconductor scintillators used on the photon counting basis. The scintillation decay time of Ga_2O_3 is much faster than those of Te-doped CdS and ZnSe.

The TSL glow curve of Ga_2O_3 is shown in Fig. 6. The measured signal is clearly distinguished from the background (BGD) signal. We confirmed that the TSL glow signal occurs at a temperature of approximately 400 °C. TSL is due to the trapping and detrapping processes of ionized charges while they travel in the sample. However, in efficient scintillators, ionized charges do not suffer such trapping processes, so that all the absorbed radiation energy is transferred to the luminescent center and fully converted into luminescence. Therefore, the observation of such notable TSL suggests that it has the potential to improve the scintillation light yield.

In conclusion, the optical, scintillation, and TSL properties of a Ga_2O_3 crystal were investigated. The emission peak near a wavelength of 380 nm was observed in both PL and scintillation spectra. The observed decay times in PL and scintillation were practically consistent. Through pulse height spectroscopy using a ^{137}Cs γ-ray source, a clear photoabsorption peak was successfully observed, and the light yield was 15000 ± 1500 photons/MeV. The scintillation decay time was 8 ns, which is the fastest among the semiconductor scintillators available for pulse height measurements using PMTs. The TSL glow curve suggests a possibility of further improvement in the scintillation properties.

Acknowledgments This research was co-supported by a Grant-in-Aid for Scientific Research (A) (26249147), and Green Photonics Research from the Ministry of Education, Culture, Sports, Science and Technology of Japan (MEXT). It is also partially supported by the Adaptable and Seamless Technology transfer Program (A-STEP) by the Japan Science and Technology Agency (JST), Murata Science Foundation, and cooperative research project of the Research Institute of Electronics, Shizuoka University.

1) T. Yanagida, J. Lumin. **169**, 544 (2016).
2) M. Kawaharada, S. Hong, M. M. Murashima, M. Kokubun, T. Itoh, K. Makishima, R. Miyawaki, H. Niko, T. Yanagida, T. Mitani, K. Nakazawa, K. Oonuki, T. Takahashi, K. Tamura, T. Tanaka, Y. Terada, Y. Fukazawa, N. Kawano, K. Kawashima, M. Ohno, K. Yamaoka, K. Abe, M. Suzuki, M. Tashiro, D. Yonetoku, and T. Murakami, Proc. SPIE **5501**, 286 (2004).
3) K. Yamaoka, M. Ohno, Y. Terada, S. Hong, J. Kotoku, Y. Okada, A. Tsutsui, Y. Endo, K. Abe, Y. Fukazawa, S. Hirakuri, T. Hiruta, K. Itoh, T. Itoh, T. Kamae, M. Kawaharada, N. Kawano, K. Kawashima, T. Kishishita, T. Kitaguchi, M. Kokubun, G. M. Madejski, K. Makishima, T. Mitani, R. Miyawaki, T. Murakami, M. M. Murashima, K. Nakazawa, H. Niko, M. Nomachi, K. Oonuki, G. Sato, M. Suzuki, H. Takahashi, I. Takahashi, T. Takahashi, S. Takeda, K. Tamura, T. Tanaka, M. Tashiro, S. Watanabe, T. Yanagida, and D. Yonetoku, IEEE Trans. Nucl. Sci. **52**, 2765 (2005).
4) T. Yanagida, A. Yoshikawa, Y. Yokota, K. Kamada, Y. Usuki, S. Yamamoto, M. Miyake, M. Baba, K. Sasaki, and M. Ito, IEEE Trans. Nucl. Sci. **57**, 1492 (2010).
5) D. Totsuka, T. Yanagida, K. Fukuda, N. Kawaguchi, Y. Fujimoto, Y. Yokota, and A. Yoshikawa, Nucl. Instrum. Methods Phys. Res., Sect. A **659**, 399 (2011).
6) Y. Shirakawa, Nucl. Instrum. Methods Phys. Res., Sect. B **263**, 58 (2007).
7) T. Yanagida, Y. Fujimoto, S. Kurosawa, K. Kamada, H. Takahashi, Y. Fukazawa, M. Nikl, and V. Chani, Jpn. J. Appl. Phys. **52**, 076401 (2013).
8) H. Wei, L. Stand, M. Zhuravleva, F. Meng, V. Martin, and C. L. Melcher, Opt. Mater. **38**, 154 (2014).
9) G. Gundiah, M. Gascón, G. Bizarri, S. E. Derenzo, and E. D. Bourret-Courchesne, J. Lumin. **159**, 274 (2015).
10) K. Watanabe, T. Yanagida, K. Fukuda, A. Koike, T. Aoki, and A. Uritani, Sens. Mater. **27**, 269 (2015).
11) T. Yanagida, Opt. Mater. **35**, 1987 (2013).
12) X. Sun, P. Gao, S. Wu, H. Wu, Q. Hu, X. Zhang, Y. Huang, and Y. Tao, Nucl. Instrum. Methods Phys. Res., Sect. B **350**, 36 (2015).
13) S. E. Derenzo, M. J. Weber, E. Bourret-Courchesne, and M. K. Klintenberg, Nucl. Instrum. Methods Phys. Res., Sect. A **505**, 111 (2003).
14) S. E. Derenzo, M. J. Weber, and M. K. Klintenberg, Nucl. Instrum. Methods Phys. Res., Sect. A **486**, 214 (2002).
15) T. Yanagida, Y. Fujimoto, and M. Koshimizu, e-J. Surf. Sci. Nanotechnol.

12, 396 (2014).
16) T. Yanagida, Y. Fujimoto, M. Miyamoto, and H. Sekiwa, Jpn. J. Appl. Phys. **53**, 02BC13 (2014).
17) T. Yanagida, M. Koshimizu, and G. Okada, Jpn. J. Appl. Phys. **55**, 02BC03 (2016).
18) D. R. Lide, *Handbook of Chemistry and Physics* (CRC Press, Boca Raton, FL, 1998).
19) Y. Fujimoto, T. Yanagida, H. Sekiwa, Y. Yokota, V. Chani, and A. Yoshikawa, Jpn. J. Appl. Phys. **50**, 01BG04 (2011).
20) L. Binet and D. Gourier, J. Phys. Chem. Solids **59**, 1241 (1998).
21) M. Zhong, Z. Wei, X. Meng, F. Wua, and J. Li, J. Alloys Compd. **619**, 572 (2015).
22) K. Sasaki, A. Kuramata, T. Masui, E. G. Villora, K. Shimamura, and S. Yamakoshi, Appl. Phys. Express **5**, 035502 (2012).
23) N. Ueda, H. Hosono, R. Waseda, and H. Kawazoe, Appl. Phys. Lett. **70**, 3561 (1997).
24) T. Onuma, S. Fujioka, T. Yamaguchi, M. Higashiwaki, K. Sasaki, T. Masui, and T. Honda, Appl. Phys. Lett. **103**, 041910 (2013).
25) Y. Oshima, E. G. Víllora, and K. Shimamura, J. Cryst. Growth **410**, 53 (2015).
26) M. Yamaga, T. Ishikawa, M. Yoshida, T. Hasegawa, E. G. Villora, and K. Shimamura, Phys. Status Solidi C **8**, 2621 (2011).
27) T. Yanagida, K. Kamada, Y. Fujimoto, H. Yagi, and T. Yanagitani, Opt. Mater. **35**, 2480 (2013).
28) T. Yanagida, Y. Fujimoto, T. Ito, K. Uchiyama, and K. Mori, Appl. Phys. Express **7**, 062401 (2014).
29) T. Yanagida, N. Kawaguchi, Y. Fujimoto, K. Fukuda, K. Watanabe, A. Yamazaki, and A. Uritani, J. Lumin. **144**, 212 (2013).
30) T. Yanagida, M. Sato, K. Kamadaa, Y. Fujimoto, Y. Yokota, A. Yoshikawa, and V. Chani, Opt. Mater. **33**, 413 (2011).
31) T. Yanagida, Y. Fujimoto, N. Kawaguchi, and S. Yanagida, J. Ceram. Soc. Jpn. **121**, 988 (2013).
32) T. Harwig, F. Kellendonk, and S. Slappendel, J. Phys. Chem. Solids **39**, 675 (1978).
33) T. Harwig and F. Kellendonk, J. Solid State Chem. **24**, 255 (1978).
34) L. Binet and J. Gourier, J. Phys. Chem. Solids **59**, 1241 (1998).
35) G. Blasse and A. Bril, J. Phys. Chem. Solids **31**, 707 (1970).
36) P. Schotanus, P. Dorenbos, and V. D. Ryzhikov, IEEE Trans. Nucl. Sci. **39**, 546 (1992).
37) C. L. Melcher and J. S. Schweitzer, IEEE Trans. Nucl. Sci. **39**, 502 (1992).